

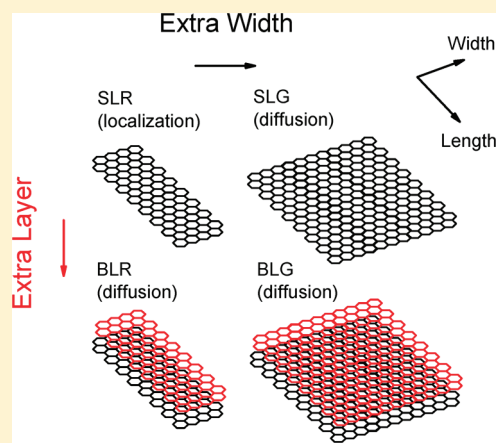
Edge Effect on Resistance Scaling Rules in Graphene Nanostructures

Guangyu Xu,^{*,†} Carlos M. Torres, Jr.,^{†,‡} Jianshi Tang,^{†,‡} Jingwei Bai,^{‡,‡} Emil B. Song,[†] Yu Huang,[‡] Xiangfeng Duan,[§] Yuegang Zhang,^{*,||} and Kang L. Wang[†][†]Department of Electrical Engineering, [‡]Department of Material Science and Engineering, [§]Department of Chemistry and Biochemistry, University of California at Los Angeles, Los Angeles, California 90095, United States^{||}Molecular Foundry, Lawrence Berkeley National Laboratory, 1 Cyclotron Road, Berkeley, California 94720, United States

S Supporting Information

ABSTRACT: We report an experimental investigation of the edge effect on the room-temperature transport in graphene nanoribbon and graphene sheet (both single-layer and bilayer). By measuring the resistance scaling behaviors at both low- and high-carrier densities, we show that the transport of single-layer nanoribbons lies in a strong localization regime, which can be attributed to an edge effect. We find that this edge effect can be weakened by enlarging the width, decreasing the carrier densities, or adding an extra layer. From graphene nanoribbon to graphene sheet, the data show a dimensional crossover of the transport regimes possibly due to the drastic change of the edge effect.

KEYWORDS: Graphene, graphene nanoribbon, resistance scaling, edge effect, dimensional crossover



Advancement of nanoscale materials has attracted considerable interest in understanding their low dimensional transport.^{1,2} Reduction of the sample size can lead to rich size-driven effects on the transport through the change of the system dimensionality.^{3,4} Graphene is an extraordinary 2D material with great potential.^{5,6} As the width of graphene narrows down to a nanometer size, graphene nanoribbon (GNR) would exhibit quasi-1D transport with the presence of an energy gap, which benefits switching on/off the devices.^{7,8} Unlike carbon nanotube with a perfectly enclosed structure,¹ as-made GNR usually has unavoidable edge disorders.⁹ The question of how the edge disorder affects GNR transport is both of fundamental interest and practical concern for device implementations.

Many efforts have been made to explore the edge effect on GNR transport, while no consensus has been reached.^{10–16} Until now, most experiments focused on the low-temperature transport in single-layer GNR (SLR) at low carrier densities. For example, Han et al. has reported the size-scaling of the SLR transport, suggesting the origin of transport gap from a combination of the edge effect and the Coulomb charging effect.¹⁰ However, their fabrication method leaves chemical coverage/residues (e.g., HSQ) on top of the samples, which makes it difficult to probe the intrinsic SLR properties. Comparatively, another work on SLRs fabricated by a metal-mask etching method attributes the size-scaling of the transport gap to the effect of charge impurities rather than that of the edge.¹¹ Given the sensitivity of the SLR to the weight of multiple types of

scatterings, it may not be surprising to see this inconsistency in the role of edge effect on transport properties, which can be quite different in samples prepared using different methods.^{11,14,15}

Length-dependence of the resistance (i.e., resistance scaling, $R-L$ relation) has been broadly used to probe the transport properties of electronic materials.^{17–20} For instance, this method has been employed to explore the electron–phonon scattering in carbon nanotubes (CNT) by comparing the $R-L$ curves under low-bias and high-bias conditions.¹⁷ Furthermore, several works have used the $R-L$ relations of CNTs to identify their transport regimes, such as the exponential $R-L$ relation and linear $R-L$ relation at localization and diffusion regimes, respectively.^{18,19} Fundamentally, the length-dependence of the resistance is a representation of the one-parameter scaling law, which has attracted much interest in understanding the phase transition in low-dimensional materials.^{20–22}

In this Letter, we aim to understand the edge effect on the room-temperature transport of GNRs and graphene sheets (with micrometer-sized width) through investigating the different resistance scaling rules in these graphene nanostructures. GNRs are fabricated by a nanowire-mask etching method with good performance as reported before.²³ For practical concerns, both off- and on-state resistance data are collected to probe the room-temperature

Received: November 12, 2010

Revised: December 29, 2010

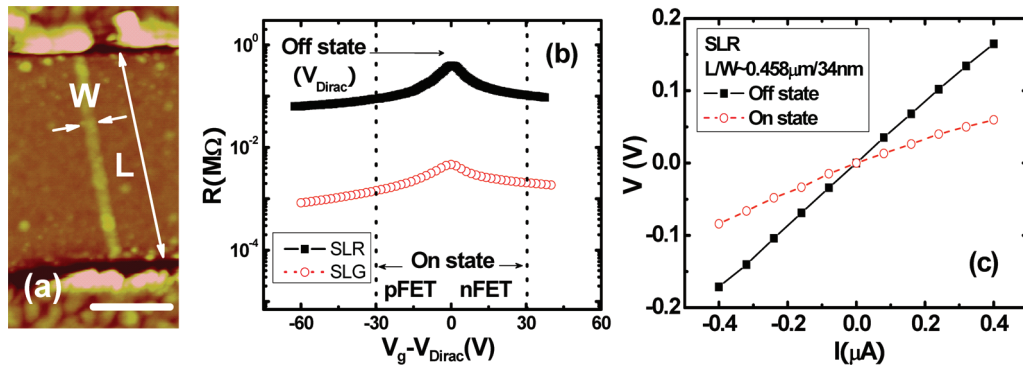


Figure 1. Typical characterization and resistance measurement of graphene nanostructures at room temperature. (a) The AFM image of a typical SLR between Ti/Au metal contacts (7/80 nm). The scale bar equals $0.3 \mu\text{m}$. (b) R vs $(V_g - V_{\text{Dirac}})$ for a SLR and a SLG with the definition of the on- and off-states. SLR is typically more resistive than SLG by 1–2 orders of magnitude. (c) Near-linear I – V curves in a SLR when the gate is biased both near and away from the Dirac point (i.e., off- and on-states, respectively).

transport at both low- and high-carrier densities. Our data show that the SLR transport lies in a strong localization regime, which can be attributed to a strong edge effect. We find that this edge effect can be weakened by enlarging the width, decreasing the carrier densities or adding an extra layer. From GNR to graphene sheet, the data exhibit a dimensional crossover of the transport regimes possibly due to the drastic change of the edge contribution. This work pinpoints the critical role of the edge effect on the crossover of the transport regimes in graphene through the resistance scaling rules; this result may provide insight on realizing scalable graphene electronics.

Our graphene sheets (with micrometer-sized width) were mechanically exfoliated from natural graphite onto a thermally grown 300 nm SiO_2 dielectric layer on a highly doped Si substrate that acts as the backside gate.⁷ Subsequently, some graphene sheets are directly patterned to Hall-bar or multiprobe devices using electron beam lithography with Ti/Au electrodes;²⁴ while some graphene sheets are first etched to GNRs by oxygen plasma using a nanowire-mask method, and then patterned into multiprobe devices.²⁵ To avoid extrinsic doping effects, (1) the nanowire-mask on top of GNRs is removed by weak sonication before the device formation; and (2) all graphene samples are maintained in vacuum and go through a baking process to desorb the contaminants before the resistance measurement. The number of graphene layers is identified through Raman spectroscopy before patterning into devices.²⁴ We thus have the samples made of single-layer and bilayer GNRs (SLR/BLR) and graphene sheets (SLG/BLG). The sample dimensions (length L) and width (W) are determined by atomic force microscopy (AFM) for GNRs²³ (see Figure 1a) and optical microscopy for graphene sheets, respectively.

DC resistance ($R = V/I$) of samples is measured within the low-bias regime at each gate bias (V_g). An ambipolar transport is typically observed (see R – V_g curves in Figure 1b) in SLR and SLG at both electron-conduction (nFET) and hole-conduction sides (pFET). To investigate the transport at both low- and high-carrier densities, we measured the resistances at both off- and on-states (i.e., R_{off} and R_{on}). Here we define (1) the off-state as V_g at the Dirac point (V_{Dirac}) (the region at low carrier densities); and (2) the on-state as V_g at $|V_g - V_{\text{Dirac}}| \sim 30 \text{ V}$ (the region at high carrier densities), where R becomes near-saturated ($<10\%$ variation with further increase of $|V_g - V_{\text{Dirac}}|$). In the experiment, we confirmed that all devices are biased in the near-linear regime at both the on- and off- states to ensure that the

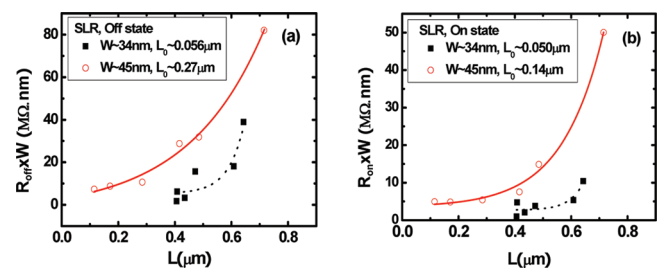


Figure 2. Resistance scaling ($R_{\text{on}}/R_{\text{off}}$ versus L) for SLR at room temperature. (a) $R_{\text{off,SLR}}$ exponentially increases with L . The fitting shows a characteristic localization length of $L_0 \sim 0.27 \mu\text{m}$ for $W \sim 45 \text{ nm}$ and $L_0 \sim 0.056 \mu\text{m}$ for $W \sim 34 \text{ nm}$, respectively. The variation of widths among samples is less than 5 nm . (b) $R_{\text{on,SLR}}$ exponentially increases with L . The fitting shows $L_0 \sim 0.14 \mu\text{m}$ for $W \sim 45 \text{ nm}$ and $L_0 \sim 0.050 \mu\text{m}$ for $W \sim 34 \text{ nm}$, respectively.

definition of R is valid (see Figure 1c). The linear I – V s for GNRs with $W > 25 \text{ nm}$ indicate that the possible Schottky-barrier near the GNR-metal contact may be smeared by temperature.^{7,11,12} In the rest of this work, we present the data from the hole-conduction side only since those from the electron-conduction side show similar trends. All resistance data are scaled by $1/W$ (i.e., RW values) for comparison among samples with different widths.

To investigate the SLR transport at low carrier densities, Figure 2a shows the length-dependence of the off resistance (i.e., $R_{\text{off}}-L$ relation) in SLRs with $W \sim 45 \text{ nm}$ and $W \sim 34 \text{ nm}$. The $R_{\text{off}}-L$ curves do not follow a linear relation ($R \propto L$), indicating that the SLR transport does not lie in a diffusive regime.^{17,19} Instead, R_{off} exhibits an exponential increase with L , featuring a transport regime of strong localization.^{15,20} The strong localization observed at room temperature indicates that the inelastic scattering is weak in our SLRs, which has been similarly found in single-walled carbon nanotube (SWNT) before.^{18,26} It is interesting to point out that both SWNT and SLR feature 1D/quasi-1D transport with a single layer of carbon atoms. Although SLRs unavoidably have edge disorders whereas SWNTs do not (structural defects are shown to result in the strong localization in SWNT¹⁸), these edge disorders can be mostly involved in the elastic scattering and contribute little to the dephasing processes.^{20,27} Fitting the data as $R(L) \sim \exp(L/L_0)$ with L_0 being the localization length,¹⁸ we find that the localization length (L_0) becomes smaller with a smaller width. This W -depen-

dence of L_0 suggests the relevance of the edge effect on the carrier localization in SLR, since the carriers in narrower SLRs are more affected by the edge.¹⁵ It has been predicted that the edge disorder can contribute to the nonuniformity of the local density-of-states, which leads to the carrier localization.^{15,16,28} In this picture, this edge effect can be stronger as W becomes smaller, resulting a stronger carrier localization with a smaller L_0 . We note that the RW value for $W \sim 45$ nm is typically larger than that for $W \sim 34$ nm, which may also relate to the significant edge effect in our SLRs.

To testify the edge effect on the carrier localization, we can compare the SLR transport at different carrier densities via the resistance scaling. This is because the edge disorders mainly contribute to the short-range scatterings, whose weight can change with the carrier densities.^{27,29,30} We thus extend the analysis to the on-state (i.e., $R_{\text{on}}-L$ relation) to describe the SLR transport at high carrier densities. Figure 2b shows that the on-state resistance (R_{on}) also exhibits an exponential $R-L$ relation with a similar W -dependence of L_0 (L_0 is smaller at a narrower W), suggesting that the edge disorder plays a role in the carrier localization at high carrier densities. For both $W \sim 45$ and 34 nm, we find that the L_0 values at the on-state are smaller than those at the off-state, indicating a stronger localization at higher carrier densities. At high carrier densities, it has been shown that the weight of edge-induced short-range scattering to the transport is larger whereas the effect of long-range disorder is insignificant due to the carrier screening.^{29,30} Hence, the trend of L_0 versus the carrier density further supports the edge effect as the main reason of the carrier localization: the edge effect is stronger at high carrier densities, leading to a stronger localization with a smaller L_0 . Conversely, the data show that long-range disorders act to weaken the localization, because their effect (long-range disorders) is stronger at low carrier densities where the localization is weaker (with a larger L_0).²⁹ The stronger carrier localization at the on-state in our SLRs supports the claim that the short-range scattering assists the carrier localization while the long-range scattering tends to delocalize it²⁷ (note: the impact of other short-range disorders away from the edges (e.g., structural defects) should be small as indicated by the negligible D-peak intensity in Raman spectroscopy). The comparison of L_0 at the on- and off-state indicates that the carrier densities affect the weight of edge effect in SLR.

So far, we attribute the resistance scaling of our SLRs to the strong localization induced by the edge effect. However, we do not exclude the possibility that SLRs fabricated by other methods can behave differently, since the weight of multiple scatterings in the fabricated SLRs can be quite different depending on the fabrication methods.¹¹ For example, HSQ-based patterning methods can leave HSQ coverage/residual which dopes the SLRs;¹⁰ top-gate structure or the coverage of the etching mask can act as an extra SLR-dielectric interface which causes scattering/screening to the carriers.^{10,31} The large variability in SLRs is similar to that of SWNTs by various growth/fabrication methods.^{18,26} In the future, the role of edge effect on resistance scaling behaviors in SLRs could be further explored by edge-engineering or changing their substrates.

We next examine the resistance scaling in BLRs. Comparing with SLR, BLR transport is not well understood yet and the experimental works are rare.^{23,32} We thus limit the discussions on the effect of the extra layer of BLR (compared to SLR) to the transport by $R-L$ relations (see Figure 3a,b). The main feature of BLR is that in contrast to SLR, the resistances of BLR at both low

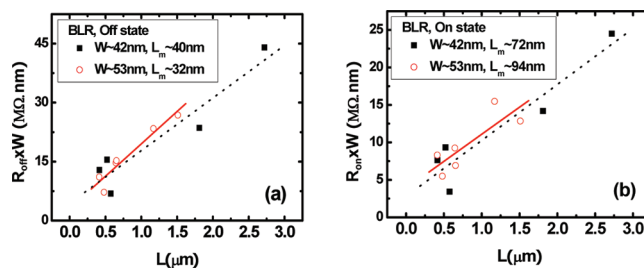


Figure 3. Resistance scaling ($R_{\text{on}}/R_{\text{off}}$ versus L) for BLR at room temperature. (a) $R_{\text{off_BLR}}$ linearly increases with L . The fitting shows a characteristic mean-free-path of $L_m \sim 40$ nm for $W \sim 42$ nm and $L_m \sim 32$ nm for $W \sim 53$ nm. The variation of widths among samples is less than 5 nm. (b) $R_{\text{on_BLR}}$ linearly increases with L . The fitting shows $L_m \sim 72$ nm for $W \sim 42$ nm and $L_m \sim 94$ nm for $W \sim 53$ nm, respectively.

and high carrier densities (R_{off} and R_{on}) exhibit a linear increase with L (i.e., $R \propto L$), characteristic of diffusive transport instead.¹⁷ For BLRs, it is suggested that the short-range edge disorder should play a more important role to the transport than SLR, since the effect of long-range disorders is weaker due to a stronger screening effect in its bilayer structure.^{30,33} Hence, the absence of localization (as indicated by the $R-L$ relation) indicates that the edge effect in BLR is weaker than that in SLR. To gain some insight on this difference, we note that some edge states of BLR have been predicted to exist only in one layer,^{34,35} the carriers on the other layer may be much less affected by these edge states. Also, the carriers in the layer with these edge states can hop to the other layer assisted by interlayer coupling.^{30,33} The effect of these edge effects can thus be weakened with the carriers being more delocalized.

To further understand the weakened edge effect in BLR, we fit the data as $\rho = dR/dL = (h/2e^2) \cdot (1/L_m)$ where L_m is the mean-free-path in the diffusive transport regime.^{17,36} The result shows that L_m at the on-state is larger than that at the off-state, indicating less carrier scatterings at higher carrier densities. We note that this trend of L_m versus the carrier density in our BLRs cannot be fully explained by the edge-induced short-range scattering, whose effect should lead to a smaller L_m at on-state as opposed to our data.^{37,38} The larger L_m at on-state in our BLRs rather appears to originate from the weakened long-range scattering at higher carrier densities similar to the case in SLR.^{29,37} Moreover, we observe a weaker W -dependence of both L_m and RW values than those in SLR (see Figure 3a,b), which also supports the weak edge effect on BLR transport. All these facts pinpoint that the edge effect in BLR is weakened by adding the extra layer, as indicated by apparently different resistance scaling rules from those in SLR.

One can expect that the edge effect in SLR and BLR could be further weakened as we significantly increase their widths to form SLG and BLG. To see if the change of edge effect can induce a crossover of the transport regimes, we studied the $R-L$ relations in SLG and BLG whose widths are typically larger than $1 \mu\text{m}$. Figure 4a shows that SLG exhibits a linear $R-L$ relation at both low and high carrier densities (R_{off} and R_{on}), featuring a diffusive transport instead of the strong localization in SLR. This dimensional crossover from quasi-1D SLR to 2D SLG reaffirms our claim that the localization in SLR is dominated by the short-range edge disorder, whose effect is much weaker in SLG. The absence of localization in SLG also indicates that the long-range disorder (as suggested being the dominant scattering in SLG)^{29,30} cannot

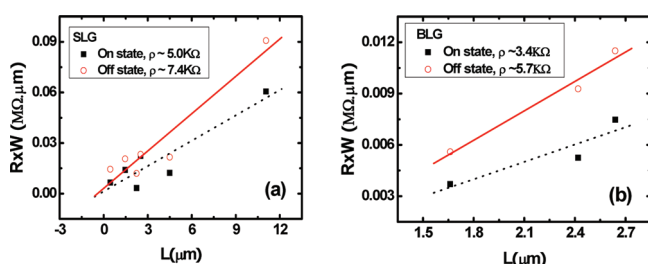


Figure 4. Resistance scaling ($R_{\text{on}}/R_{\text{off}}$ versus L) for SLG and BLG at room temperature. (a) Both $R_{\text{on_SLG}}$ and $R_{\text{off_SLG}}$ linearly increase with L and have a fitted resistivity of $\rho_{\text{on_SLG}} \sim 5.0 \text{ K}\Omega$ and $\rho_{\text{off_SLG}} \sim 7.4 \text{ K}\Omega$, respectively. (b) Both $R_{\text{on_BLG}}$ and $R_{\text{off_BLG}}$ linearly increase with L and have a fitted resistivity of $\rho_{\text{on_BLG}} \sim 3.4 \text{ K}\Omega$ and $\rho_{\text{off_BLG}} \sim 5.7 \text{ K}\Omega$, respectively.

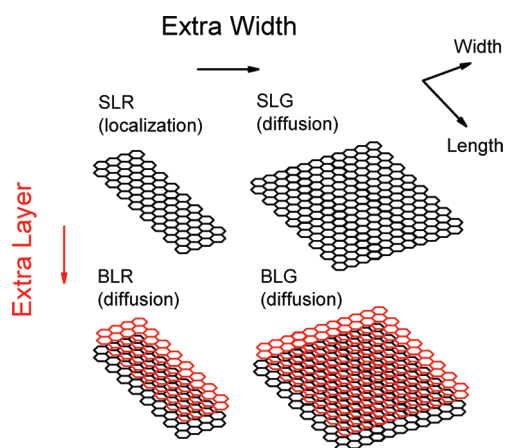


Figure 5. Schematics for the crossover of transport regimes in graphene nanostructures. The edge effect in SLR can be weakened by either adding an extra layer to form BLR or increasing the width to form SLG; both cause the transition of transport regimes from localization to diffusion. Note that the carrier densities can also affect the edge effect in SLR, which can be tuned by gate biases.

lead to the carrier localization. Figure 4b shows that BLG also features a diffusive transport as indicated by the linear R – L relations at both the on- and off-states. This can be explained as BLG having an even weaker edge effect (due to the large width) than BLR; hence neither can form the localization. We fit the SLG and BLG data as $\rho_{2D} = d(RW)/dL$ according to the 2D diffusive transport.³⁹ The obtained ρ_{2D} values are reasonable for SLG and BLG with the hole mobility ~ 1000 – $6000 \text{ cm}^2/(\text{V}\cdot\text{s})$ (see Figure 4a,b).⁴⁰

In summary, we present the resistance scaling in both quasi-1D and 2D graphene materials (SLR, BLR, SLG, BLG, see Figure 5), which pinpoints the critical role of the edge effect on the crossover of the transport regimes. By measuring the R – L relation at both low and high carrier densities, we find that the SLR transport lies in the strong localization regime, which can be mainly attributed to the effect of edge-disorders. Through the comparisons among the four graphene nanostructures, we find that the edge effect on the graphene transport can be weakened by enlarging the width, decreasing the carrier densities or adding an extra layer. Our results reveal the critical role of edge effect on graphene transport and thus the resistance scaling rules, which may provide insight to realize the ultimate goal of scalable graphene electronics.

■ ASSOCIATED CONTENT

S Supporting Information. Graphene sheet sample preparation (large width), graphene nanoribbon sample preparation, resistance measurement, sample dimension (length and width) measurement, length-dependence of $R_{\text{off}}/R_{\text{on}}$ in four graphene nanostructures, and additional references. This material is available free of charge via the Internet at <http://pubs.acs.org>.

■ AUTHOR INFORMATION

Corresponding Author

*E-mail: guangyu@ee.ucla.edu (GX); y Zhang5@lbl.gov (YZ).

Author Contributions

[†]These authors contributed equally to this work

■ ACKNOWLEDGMENT

The authors thank F. Miao, X. Zhang, R. Cheng, and L. Liao for helpful discussions. We especially thank M. Y. Han from P. Kim's group for theoretical discussions. We greatly appreciate technical support from M. Wang, C. Zeng, S. Aloni, and T. Kuykendall. This work was in part supported by MARCO Focus Center on Functional Engineered Nano Architectonics and the U.S. Department of Energy under Contract No. DE-AC02-05CH11231.

■ REFERENCES

- (1) Avouris, P.; Chen, Z.; Perebeinos, V. Carbon-based electronics. *Nat. Nanotechnol.* **2007**, *2*, 605–615.
- (2) Salvatore-Arico, A.; Bruce, P.; Scrosati, B.; Tarascon, J.-M.; van Schalkwijk, W. Nanostructured materials for advanced energy conversion and storage devices. *Nat. Mater.* **2005**, *4*, 366–377.
- (3) Yi Zhang; et al. Crossover of the three-dimensional topological insulator Bi_2Se_3 to the two-dimensional limit. *Nat. Phys.* **2010**, *6*, 584–588.
- (4) Xu, K.; Qin, L.; Heath, J. R. The crossover from two dimensions to one dimension in granular electronic materials. *Nat. Nanotechnol.* **2009**, *4*, 368–372.
- (5) Geim, A. K. Graphene: status and prospects. *Science* **2009**, *324*, 1530–1534.
- (6) Lin, Y.-M.; et al. 100-GHz Transistors from Wafer-Scale Epitaxial Graphene. *Science* **2010**, *327*, 662.
- (7) Han, M. Y.; Özyilmaz, B.; Zhang, Y.; Kim, P. Energy band-gap engineering of graphene nanoribbons. *Phys. Rev. Lett.* **2007**, *98*, No. 206805.
- (8) Chen, Z.; Lin, Y.-M.; Rooks, M. J.; Avouris, P. Graphene Nano-Ribbon Electronics. *Physica E* **2007**, *40*, 228–232.
- (9) Tapasztó, L.; Dobrik, G.; Lambin, P.; Biro, L. P. Tailoring the atomic structure of graphene nanoribbons by scanning tunneling microscope lithography. *Nat. Nanotechnol.* **2008**, *3*, 397–401.
- (10) Han, M. Y.; Brant, J. C.; Kim, P. Electron transport in disordered graphene nanoribbons. *Phys. Rev. Lett.* **2010**, *104*, No. 056801.
- (11) Gallagher, P.; Todd, K.; Goldhaber-Gordon, D. Disorder-induced gap behavior in graphene nanoribbons. *Phys. Rev. B* **2010**, *81*, No. 115409.
- (12) Liu, X.; Oostinga, J. B.; Morpurgo, A. F.; Vandersypen, L. M. K. Electrostatic confinement of electrons in graphene nanoribbons. *Phys. Rev. B* **2010**, *80*, No. 121407 (R).
- (13) Stampfer, C.; et al. Energy gaps in etched graphene nanoribbons. *Phys. Rev. Lett.* **2009**, *102*, No. 056403.
- (14) Poumirol, J. M.; et al. Edge magnetotransport fingerprints in disordered graphene nanoribbons. *Phys. Rev. B* **2010**, *82*, No. 041413.

- (15) Evaldsson, M.; Zozoulenko, I. V.; Xu, H.; Heinzl, T. Edge-disorder-induced Anderson localization and conduction gap in graphene nanoribbons. *Phys. Rev. B* **2008**, *78*, No. 161407 (R).
- (16) Mucciolo, E. R.; Castro Neto, A. H.; Lewenkopf, C. H. Conduction quantization and transport gaps in disordered graphene nanoribbons. *Phys. Rev. B* **2009**, *79*, No. 075407.
- (17) Park, J.-Y.; Rosenblatt, S.; Yaish, Y.; Sazonova, V.; Ustunel, H.; Braig, S.; Arias, T. A.; Brouwer, P. W.; McEuen, P. L. Electron-Phonon Scattering in Metallic Single-Walled Carbon Nanotubes. *Nano Lett.* **2004**, *4*, 517–520.
- (18) Gomez-navarro, C.; De Pablo, P. J.; Gomez-Herrero, J.; Biel, B.; Garcia-Vidal, F. J.; Rubio, A.; Flores, F. Tuning the conductance of single-walled carbon nanotube by ion irradiation in Anderson localization regime. *Nat. Mater.* **2005**, *4*, 534–539.
- (19) Purewal, M. S.; Hong, B. H.; Ravi, A.; Chandra, B.; Hone, J.; Kim, P. Scaling of resistance and electron mean free path of single-walled carbon nanotubes. *Phys. Rev. Lett.* **2007**, *98*, No. 186808.
- (20) Lherbier, A.; Biel, B.; Niquet, Y.-M.; Roche, S. Transport length scales in disordered graphene-based materials: strong localization regimes and dimensionality effects. *Phys. Rev. Lett.* **2008**, *100*, No. 036803.
- (21) Bardarson, J. H.; Tworzydło, J.; Brouwer, P. W.; Beenakker, C. W. J. One-Parameter Scaling at the Dirac Point in Graphene. *Phys. Rev. Lett.* **2007**, *99*, No. 106801.
- (22) Bodyfelt, J. D.; Kottos, T.; Shapiro, B. One-Parameter Scaling Theory for Stationary States of Disordered Nonlinear Systems. *Phys. Rev. Lett.* **2010**, *104*, No. 164102.
- (23) Xu, G.; et al. Low-noise submicron channel graphene nanoribbons. *Appl. Phys. Lett.* **2010**, *97*, No. 073107.
- (24) Xu, G.; Torres, C. M., Jr.; Zhang, Y.; Liu, F.; Song, E. B.; Wang, M.; Zhou, Y.; Zeng, C.; Wang, K. L. Effect of Spatial Charge Inhomogeneity on $1/f$ Noise Behavior in Graphene. *Nano Lett.* **2010**, *10*, 3312–3317.
- (25) Bai, J.; Duan, X.; Huang, Y. Rational Fabrication of Graphene Nanoribbons Using a Nanowire Etch Mask. *Nano Lett.* **2009**, *9*, 2083–2087.
- (26) Sundqvist, P.; et al. Voltage and Length-Dependent Phase Diagram of the Electronic Transport in Carbon Nanotubes. *Nano Lett.* **2007**, *7*, 2568–2573.
- (27) Tikhonenko, F. V.; Kozikov, A. A.; Savchenko, A. K.; Gorbahev, R. B. Transition between electron localization and anti-localization in graphene. *Phys. Rev. Lett.* **2009**, *103*, No. 226801.
- (28) Sols, F.; et al. Coulomb blockade in graphene nanoribbons. *Phys. Rev. Lett.* **2007**, *99*, No. 166803.
- (29) Adam, S.; Hwang, E. H.; Rossi, E.; Das Sarma, S. Theory of charged impurity scattering in two-dimensional graphene. *Solid State Commun.* **2009**, *149*, 1072–1079.
- (30) Sarma, S. D.; Hwang, E. H.; Rossi, E. Theory of carrier transport in bilayer graphene. *Phys. Rev. B* **2010**, *81*, No. 161407(R).
- (31) Bai, J.; et al. Very large magnetoresistance in graphene nanoribbons. *Nat. Nanotechnol.* **2010**, *5*, 655–659.
- (32) Xu, H.; Heinzl, T.; Zozoulenko, I. V. Edge disorder and localization regimes in bilayer graphene nanoribbons. *Phys. Rev. B* **2009**, *80*, No. 045308.
- (33) Sui, Y.; Appenzeller, J. Screening and interlayer coupling in multilayer graphene field-effect transistors. *Nano Lett.* **2009**, *9*, 2973–2977.
- (34) Castro, E. V.; Peres, N. M. R.; Lopes dos Santos, J. M. B.; Castro Neto, A. H.; Guinea, F. Localized states at zigzag edges of bilayer graphene. *Phys. Rev. Lett.* **2008**, *100*, No. 026802.
- (35) Castro, E. V.; Lopez-Sancho, M. P.; Vozmediano, M. A. New type of vacancy-induced localized states in multilayer graphene. *Phys. Rev. Lett.* **2010**, *104*, No. 036802.
- (36) Areshkin, D. A.; Gunlycke, D.; White, C. T. Ballistic transport in graphene nanostrips in the presence of disorder: Importance of edge effect. *Nano Lett.* **2007**, *7*, 204–210.
- (37) Du, X.; Skachko, I.; Barker, A.; Andrei, E. Y. Approaching ballistic transport in suspended graphene. *Nat. Nanotechnol.* **2008**, *3*, 491–495.
- (38) Other possible reasons such as the gate-induced bandgap opening in BLR may also affect the L_m values at high carrier densities.^{24,32} However, direct experimental evidence of this bandgap-opening effect in BLR is still lacking at room temperature.
- (39) We fit the SLG and BLG data from the samples with different widths since their RW values have weak W -dependence. For example, we find that both SLGs with $L/W \sim 11.1 \mu\text{m}/6 \mu\text{m}$ and $L/W \sim 11.1 \mu\text{m}/8 \mu\text{m}$ exhibit similar RW values $\sim 0.5 \text{ M}\Omega \cdot \mu\text{m}$ at the on-state and $0.9 \text{ M}\Omega \cdot \mu\text{m}$ at the off-state, respectively.
- (40) Castro Neto, A. H.; Guinea, F.; Peres, N. M. R.; Novoselov, K. S.; Geim, A. K. The electronic properties of graphene. *Rev. Mod. Phys.* **2009**, *81*, 109–162.